*Appl. Sci.* **2015**, *5*, 1484-1493; doi:10.3390/app5041484

OPEN ACCESS

*applied sciences*

**ISSN 2076-3417**

www.mdpi.com/journal/applsci

*Article*

# Trichromatic $\pi$-Pulse for Ultrafast Total Inversion of a Four-Level Ladder System

**Carles Serrat [1,*], Montserrat Corbera [2] and John Afa [1]**

[1] Departament de Física, Universitat Politècnica de Catalunya, Colom 11, Terrassa (Barcelona) 08222, Spain; E-Mail: iduabo.john.afa@alu-etsetb.upc.edu

[2] Escola Politècnica Superior, Universitat de Vic, Carrer de la Laura 13, Vic (Barcelona) 08500, Spain; E-Mail: montserrat.corbera@uvic.cat

* Author to whom correspondence should be addressed; E-Mail: carles.serrat-jurado@upc.edu; Tel.: +34-93-739-8137; Fax: +34-93-739-8000.

Academic Editor: Totaro Imasaka

*Received: 8 October 2015 / Accepted: 24 November 2015 / Published: 30 November 2015*

---

**Abstract:** We present a numerical solution for complete population inversion in a four-level ladder system obtained by using a full $\pi$-pulse illumination scheme with resonant ultrashort phase-locked Gaussian laser pulses. We find that a set of pulse areas such as $\sqrt{3}\pi$, $2\pi$, and $\sqrt{3}\pi$ completely inverts the four-level system considering identical effective dipole coupling coefficients. The solution is consistent provided the involved electric fields are not too strong and it is amply accurate also in the case of diverse transition dipole moments. We study the effect of detuning and chirp of the laser pulses on the complete population inversion using the level structure of atomic sodium interacting with ps and fs pulses as an example. Our result opens the door for multiple applications such as efficient ultrashort pulse lasing in the UV or the engineering of quantum states for quantum computing.

**Keywords:** ultrashort pulses; coherent control; quantum computing

---

## 1. Introduction

Control of population transfer in multiphoton transitions in atoms and molecules with laser pulses is a fundamental tool that has been extensively investigated in quantum optics since the advent of ultrashort pulses due to its value in several areas, including nonlinear spectroscopy [1], femtochemistry and biology [2], or in quantum information and in the quantum engineering of light states [3], where quantum systems need to be fully controlled. Several techniques have been reported for control of population transfer between a pair of quantum states involving multiphoton transitions, such as spectral shaping of the fields illuminating the medium [4,5], adiabatic methods [6–9] and $\pi$-pulse polychromatic control [10–13].

The coherent interaction between a three-level system and two fields has been studied theoretically for different processes [14–21]. In a three-level ladder system with resonant fields the solution for $\pi$-pulse bichromatic control is analytical [17]. The pulse area for complete transfer of the occupation probability from the ground state to the highest state is in this case $\sqrt{2}\pi$ for both fields, with the pulse area defined as $\int_{-\infty}^{\infty} \Omega(t)dt$, where $\Omega(t) = \mu E(t)/\hbar$ is the Rabi frequency of the transition, $\mu$ is the electric dipole moment and $E(t)$ is the electric field amplitude of the laser pulse. The analysis of coupled differential equations arising from coherent multiphoton interactions however, even in simple multilevel quantum systems, is a complex task that often leads to expressions that lack any physical insight, so that very few have addressed the general problem analytically [22]. It is therefore desirable to develop efficient numerical algorithms for the solution of the more complicated systems.

For the case of a four-level ladder system, population transfer schemes combining adiabatic and $\pi$-pulse techniques have been proposed [23]. Full $\pi$-pulse polychromatic control techniques are however preferred in some cases because the intensities required for optimal excitation are on the order of the intensities for resonantly pumped single-photon transitions, and therefore they result energetically more efficient than adiabatic methods. In this paper we present a numerical solution for complete population inversion in a four-level ladder system by using full $\pi$-pulse control.

## 2. Numerical Simulations

We have solved numerically the Liouville equations for a four-level ladder system coherently interacting with a tricolor pulse without the assumptions of the rotating-wave approximation (RWA). Avoiding the RWA in the density-matrix formalism allows to account for the interaction of all the Fourier components of the pulses with all the permitted transitions in the system, and therefore in our study we can evaluate the effect of large detuning and chirp of ultrashort pulses with a broad range of intensities. The density matrix equations that we numerically solve are as follows [24].

$$
\begin{aligned}
\dot{\rho}_{22} &= -\gamma_{22}\rho_{22} + \gamma_{32}\rho_{33} + \gamma_{42}\rho_{44} + i\frac{E(t)}{\hbar}(\mu_{12}(\rho_{12}-\rho_{21}) + \mu_{23}(\rho_{32}-\rho_{23})) \\
\dot{\rho}_{33} &= -\gamma_{33}\rho_{33} + \gamma_{43}\rho_{44} + -i\frac{E(t)}{\hbar}(\mu_{23}(\rho_{32}-\rho_{23}) + \mu_{34}(\rho_{34}-\rho_{43})) \\
\dot{\rho}_{44} &= -\gamma_{44}\rho_{44} + i\frac{E(t)}{\hbar}(\mu_{14}(\rho_{14}-\rho_{41}) + \mu_{34}(\rho_{34}-\rho_{43})) \\
\dot{\rho}_{11} &= -\dot{\rho}_{33} - \dot{\rho}_{22} - \dot{\rho}_{44} \\
\dot{\rho}_{12} &= -\bar{\Gamma}_{12}\rho_{12} + i\omega_{12}\rho_{12} + i\frac{E(t)}{\hbar}(\mu_{12}(\rho_{22}-\rho_{11}) + \mu_{14}\rho^{*}_{24} - \mu_{23}\rho_{13}) \\
\dot{\rho}_{13} &= -\bar{\Gamma}_{13}\rho_{13} + i\omega_{13}\rho_{13} + i\frac{E(t)}{\hbar}(\mu_{12}\rho_{23} - \mu_{23}\rho_{12} + \mu_{14}\rho^{*}_{34} - \mu_{34}\rho_{14}) \\
\dot{\rho}_{14} &= -\bar{\Gamma}_{14}\rho_{14} + i\omega_{14}\rho_{14} + i\frac{E(t)}{\hbar}(\mu_{14}(\rho_{44}-\rho_{11}) - \mu_{34}\rho_{13} + \mu_{12}\rho_{24}) \\
\dot{\rho}_{23} &= -\bar{\Gamma}_{23}\rho_{23} + i\omega_{23}\rho_{23} + i\frac{E(t)}{\hbar}(\mu_{23}(\rho_{33}-\rho_{22}) - \mu_{34}\rho_{24} + \mu_{12}\rho_{13}) \\
\dot{\rho}_{24} &= -\bar{\Gamma}_{24}\rho_{24} + i\omega_{24}\rho_{24} + i\frac{E(t)}{\hbar}(\mu_{12}\rho_{14} - \mu_{14}\rho^{*}_{12} + \mu_{23}\rho_{34} - \mu_{34}\rho_{23}) \\
\dot{\rho}_{34} &= -\bar{\Gamma}_{34}\rho_{34} + i\omega_{34}\rho_{34} + i\frac{E(t)}{\hbar}(\mu_{34}(\rho_{44}-\rho_{33}) + \mu_{23}\rho_{24} - \mu_{14}\rho^{*}_{13})
\end{aligned}
\tag{1}
$$

where $\rho_{ii}$ are the populations of the levels $i$, the off-diagonal elements $\rho_{ij}$ represent the coherences between levels $i, j$, $\mu_{ij}$ are the dipole coupling coefficients of the corresponding electronic transitions, and $\omega_{ij} = (\epsilon_j - \epsilon_i)/\hbar$ are the angular frequencies of the transitions $i-j$, with $\epsilon_i$ being the energies of the corresponding quantum states. The decay rates of the transitions $i-j$ are given by $\gamma_{ij}$, and the population relaxation rates of the levels satisfy $\gamma_{22} = \gamma_{21}$, $\gamma_{33} = \gamma_{31} + \gamma_{32}$, $\gamma_{44} = \gamma_{41} + \gamma_{42} + \gamma_{43}$. The overall rate $\gamma_{ii}$, which is inversely proportional to the population decay time $T_1$ of level $i$ ($T_1 = \gamma_{ii}^{-1}$), is thus given by the sum of each deactivation pathway in the four-level system. The decay rates of the coherences are defined by $\bar{\Gamma}_{12} = \gamma_{22}/2 + \Gamma_{12}$, $\bar{\Gamma}_{13} = \gamma_{33}/2 + \Gamma_{13}$, $\bar{\Gamma}_{14} = \gamma_{44}/2 + \Gamma_{14}$, $\bar{\Gamma}_{23} = (\gamma_{22} + \gamma_{33})/2 + \Gamma_{23}$, $\bar{\Gamma}_{24} = (\gamma_{22} + \gamma_{44})/2 + \Gamma_{24}$ and $\bar{\Gamma}_{34} = (\gamma_{33} + \gamma_{44})/2 + \Gamma_{34}$, which include the relaxation of the coherences and the pure coherence dephasing rates $\Gamma_{ij}$, which are defined as the inverse of the corresponding pure coherence dephasing times ($\Gamma_{ij} = T_2^{-1}$). The laser pulses used in our simulations are of Gaussian shape, with the electric field $E(t)$ given by

$$
E(t) = E_1(t) + E_2(t) + E_3(t) = e^{-(t/\tau)^2}\{E_{01}\cos(\omega_1 t) + E_{02}\cos(\omega_2 t) + E_{03}\cos(\omega_3 t)\} \tag{2}
$$

where $E_{01}$, $E_{02}$ and $E_{03}$ are the peak amplitudes of the three pulse components $E_1(t)$, $E_2(t)$ and $E_3(t)$, and $\omega_1$, $\omega_2$ and $\omega_3$ are the respective optical angular frequencies. The duration of the pulses is given by $\tau = t_p/(\sqrt{2\ln 2})$, where $t_p$ is the full width at half maximum of the pulse intensity profile. In the present study we consider ultrashort pulses of ps and fs durations, so that considering an effective dipole coupling coefficient such as $\mu \sim 10^{-29}$ Cm for all transitions, the peak intensities for $2\pi$ pulses of 10 ps and 100 fs durations result in $\sim 10^5$ W/cm$^2$ and $\sim 10^{10}$ W/cm$^2$, respectively.

The level structure that we have chosen in our simulations corresponds to the energy levels of sodium $^{23}_{11}$Na, in particular our ground state represents the sodium $3s$ state, the intermediate states are the $3p$ and $4s$ states, and the upper state is the $7p$ state. We numerically integrate Equation (1) with an algorithm

based on a 4–5 order Runge-Kutta solver which scans the areas of the three pulse components $E_1(t)$, $E_2(t)$ and $E_3(t)$ between 0 to $4\pi$ in steps of $0.01\pi$. Starting with the system in the ground $3s$ state the goal is to obtain complete population transfer to the $7p$ state. We first consider a trichromatic pulse with a duration of 10 ps composed of three resonant components with central wavelengths of 589 nm, 1141 nm and 781 nm (see Figure 1). We obtain that the only solution for total population transfer from the ground state $3s$ to the highest state $7p$ is the set of pulse areas $\sqrt{3}\pi$, $2\pi$, and $\sqrt{3}\pi$, as it is illustrated in Figure 1. As it is shown in Figure 1, the intermediate levels $3p$ and $4s$ are temporally occupied during the interaction process, but at the end of the interaction all the population is efficiently transferred to the $7p$ state. By varying the area of pulses $E_1(t)$ and $E_3(t)$ in a 4% we obtain that the population transfer to the $7p$ state is reduced to roughly 98%, which gives an estimation of the accuracy of our result. In the inset of Figure 1 we show how doubling the area of each pulse the $2\pi$-pulse effect is retrieved, with all the population being back to the ground state at the end of the interaction.

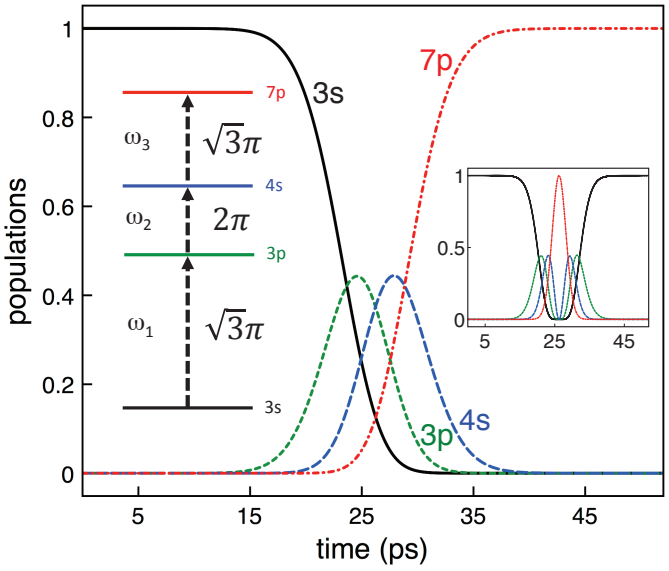


**Figure 1.** Time evolution of the populations of the four levels, as indicated, for a "$\pi$-pulse" transition produced by a tricolor resonant 10 ps Gaussian pulse of central angular frequencies $\omega_1$, $\omega_2$ and $\omega_3$. The inset on the left shows a scheme of the four-level ladder system with the pulse areas that completely invert the population. Atomic sodium has been considered in our study as an example, with transition energies such as $\omega_{12} = \omega_1 = 16,978$ cm$^{-1}$ (589 nm for $3s$–$3p$), $\omega_{23} = \omega_2 = 8762$ cm$^{-1}$ (1141 nm for $3p$–$4s$), and $\omega_{34} = \omega_3 = 12,801$ cm$^{-1}$ (781 nm for $4s$–$7p$). The inset on the right shows a complete oscillation of a "$2\pi$-pulse", which is produced with the corresponding double pulse areas $2\sqrt{3}\pi$, $4\pi$, and $2\sqrt{3}\pi$.

The solution that we report can be scaled to other pulse durations, which is also described in the case of a three-level ladder system [12]. Indeed, we find that complete population inversion is reproduced for pulses longer than 10 ps and also for shorter pulses. The limitation of the result is determined, on the one hand, on the relaxation times and line-broadening factors of the system, which prevent the usability of long pulses, and on the other hand, on the value of the transition dipole moments combined with the duration of the pulse, since weak coupling dipole moments with ultrashort pulses

result in large peak intensities involving carrier field dynamics [26] and ac-Stark shifts that preclude the population inversion effect. As an example, for values of the transition dipole moments in sodium as $\mu_{3s-3p} = 2.11 \times 10^{-29}$ Cm, $\mu_{3p-4s} = 2.09 \times 10^{-29}$ Cm, and $\mu_{4s-7p} = 1.32 \times 10^{-30}$ Cm, and considering 10 ps laser pulses, the peak intensity of the corresponding laser pulses for $\sqrt{3}\pi$, $2\pi$, and $\sqrt{3}\pi$ illumination is $I_1 = 4.3 \times 10^5$ W/cm$^2$, $I_2 = 5.8 \times 10^5$ W/cm$^2$, $I_3 = 1.1 \times 10^8$ W/cm$^2$, which results in a population inversion to the $7p$ state of 99.3%. This population inversion is reduced to 98% for 5 ps pulses and to 84% for 1 ps pulses, which require pulse peak intensities of two more orders of magnitude. Dephasing times of the considered transitions in sodium are in general of the order of ns and therefore they do not influence the results obtained in the present study, which considers ps and fs pulses, but as commented above the complete density matrix equations including dephasing rates need to be computed for longer pulses.

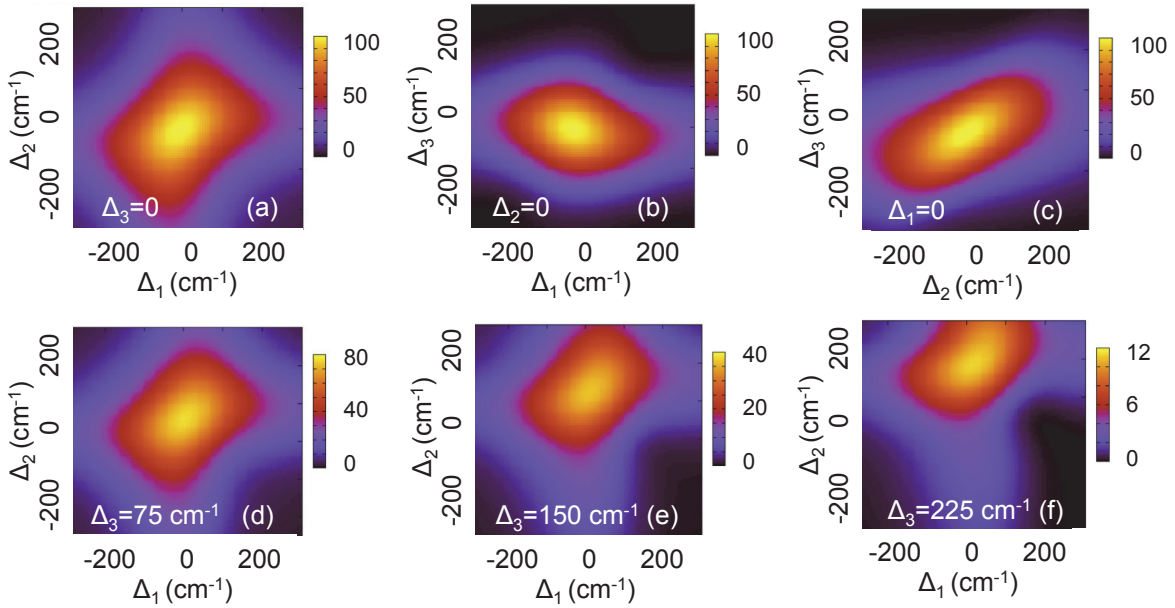


**Figure 2.** Study of the effect of field detuning on the population inversion from level $3s$ to level $7p$ in atomic sodium (see Figure 1) for 100 fs pulses. Note that in (**a**–**c**) the most yellow regions correspond to 100% population transfer; while in (**d**–**f**), they correspond to 80%, 40% and 12%, respectively.

We have investigated the robustness of the full $\pi$-pulse trichromatic scheme against detuning and chirp of the laser pulses by considering different pulse durations. In order to study the effect of field detuning we define the following detuning parameters: $\Delta_1 = \omega_{12} - \omega_1$, $\Delta_2 = \omega_{12} + \omega_{23} - \omega_1 - \omega_2$ and $\Delta_3 = \omega_{12} + \omega_{23} + \omega_{34} - \omega_1 - \omega_2 - \omega_3$, with $\omega_{ij}$ corresponding to the energy transition of the $i, j$ levels ($1 \equiv 3s$, $2 \equiv 3p$, $3 \equiv 4s$, $4 \equiv 7p$, see Figure 1). $\Delta_3 = 0$ corresponds to all field detunings that keep the three-photon resonance between levels $7p$ and $3s$, $\Delta_2 = 0$ means that the two-photon resonance between $3s$ and $4s$ is maintained, and $\Delta_1 = 0$ means that the $E_1$ field is in resonance with the $3s$–$3p$ transition. Figure 2 shows how complete population inversion from level $3s$ to level $7p$ is affected by detuning in the case of using 100 fs pulses. Figure 2a shows the results obtained when the three-photon resonance between $3s$ and $7p$ is kept ($\Delta_3 = 0$). In the case shown in Figure 2b the two-photon resonance between $3s$

and $4s$ is maintained while the frequency of the three pulses is varied ($\Delta_2 = 0$). In Figure 2c the results corresponding to having resonance in the lowest transition $3s$–$3p$ are shown ($\Delta_1 = 0$). In these three first cases we observe a roughly symmetrical geometry around the center of the figure where the detuning is zero ($\Delta_1 = \Delta_2 = \Delta_3 = 0$), which shows the sensitivity of the complete inversion effect. We observe that for inversion to stay at values larger than 95% the system supports detuning of the order of about 100 cm$^{-1}$, which roughly corresponds to the width of the Gaussian 100 fs pulses used (147 cm$^{-1}$). In Figure 2d–f the three detuning parameters have been varied simultaneously. Figure 2d shows that for $\Delta_3 = 75$ cm$^{-1}$ a comparable detuning $\Delta_2$ produces a population inversion as high as 80%. The combined effect of $\Delta_2$ and $\Delta_3$ is further shown in Figure 2e for a higher value of $\Delta_3 = 150$ cm$^{-1}$, where a corresponding higher value of $\Delta_2$ reduces the inversion to about 40%. For larger values of $\Delta_3$ population inversion is basically suppressed, as it is shown in Figure 2f, where the yellow color in the plot represents only a 12% of inversion. For longer pulses the supported detuning is scaled accordingly with the duration of the pulses, as it was also reported in the case of a three-level system interacting with two phase-locked pulses [12]. This is, if a factor $m$ is multiplied to the duration of the pulse, the same factor $m$ divides the scale of the supported detuning, which concurs with the fact the detuning should be comparable to the spectral width of the pulses. The optimal pulse duration for a particular application and the corresponding effect of detuning will therefore be dependent basically on the line-broadening factors of the system under consideration and the value of the dipole moments of the transitions, which for ultrafast population inversion have to be high enough not to involve too strong laser fields, as commented above.

We next have considered pulse chirp on the three pulses interacting with the four-level system and have computed its effect for different transform limited (TL) pulse durations. In Figure 3 the effect of pulse chirp on the final populations is shown. The populations of the four levels after the pulse interaction are plotted as a function of the spectral chirp parameter $\varphi''$, which has been implemented in the Fourier domain as $\varphi(\omega) = 0.5\varphi''(\omega - \omega_0)^2$, with $\varphi(\omega)$ being the group delay dispersion (GDD) added to the spectral phase of the pulse. We note that, as only the spectral phase of the laser pulse is varied in our study, the frequency content remains as the TL pulse for any value of the spectral chirp $\varphi''$. The rephasing of the spectral components produces a time broadening of the pulse given by $t_{p_c} = \sqrt{t_p^4 + 16(\ln 2)^2\varphi''^2}/t_p$, where $t_{p_c}$ is the full width at half maximum of the chirped pulse intensity profile [22], and therefore we implement the regular effect produced by for instance propagating the laser pulse in a linear dispersive medium. For GDD measurements of atmospheric and other gases with ultrashort pulses see, e.g., [27].

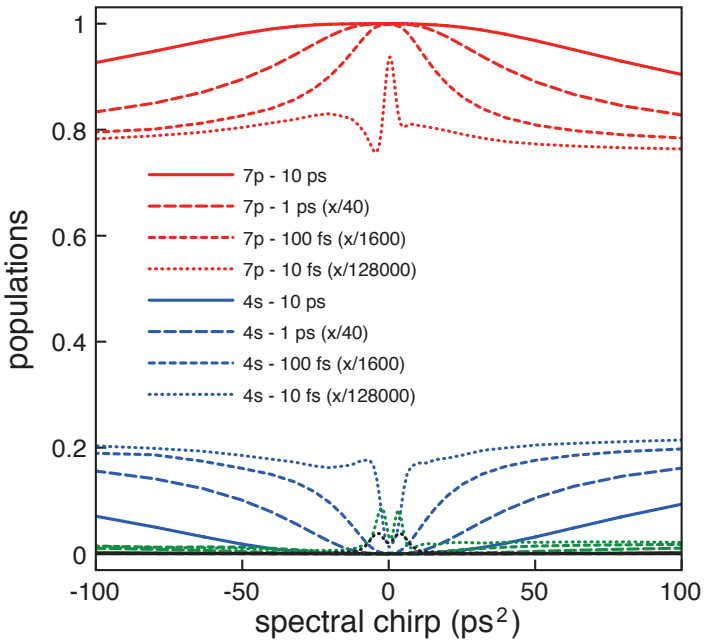


**Figure 3.** Effect of pulse chirp $\varphi''$ on the populations of the four levels after the interaction for different durations of the corresponding TL pulses. Indicated are the final populations of levels $7p$ (red lines) and $4s$ (blue lines); levels $3p$ and $3s$ become basically unpopulated in all cases (green and black lines). Note that the $x$-axis has been scaled for the different cases as indicated in the legend of the figure. Clearly, the population inversion produced by the longer pulses is less affected by chirp.

**Table 1.** Effect of GDD.

| $t_p$ | $\varphi''$ | $t_{p_c}$ | % Inversion |
|---|---|---|---|
| 10 ps | 100 ps$^2$ | 29.5 ps | $\approx 92\%$ |
| 1 ps | 0.94 ps$^2$ | 2.8 ps | $\approx 92\%$ |
| 100 fs | 9765 fs$^2$ | 289 fs | $\approx 92\%$ |

In our study we have considered the same amount of spectral chirp for the three frequency components of the interacting pulse and with central frequencies resonant to their closest transition ($\omega_1 = \omega_{12}$, $\omega_2 = \omega_{23}$, $\omega_3 = \omega_{34}$). The red lines in Figure 3 correspond to the final population in level $7p$, the blue lines show the final population in level $4s$, and the green and black lines (close to zero) are the final populations in levels $3p$ and $3s$. It is clear from Figure 3 that the main effect of pulse chirp in the case that we have considered is to bring part of the final population to level $4s$, while levels $3p$ and $3s$ remain basically unpopulated. Note that the $x$-axis in Figure 3 have been scaled for the different pulse durations, as it is indicated in the legend of the figure. We observe that the trichromatic $\pi$-pulse effect is robust for spectral chirps of the order of ps$^2$ for TL pulses of 10 ps. In Table 1 we show the GDD ($\varphi''$) values supported for the pulses with TL durations of $t_p$ = 1 ps, 10 ps and 100 fs for a reduction in the population inversion to values of $\approx 92\%$, together with the associated pulse broadening ($t_{p_c}$). Clearly, the shorter

pulses support a lower value of chirp, with a pulse broadening that corresponds roughly to three times the TL duration for the three cases. We finally observe that the large electric fields associated to shorter pulses of the considered pulse areas prevent complete population inversion, as shown for the case of 10 fs pulses by the red-dotted line in Figure 3.

## 3. Conclusions

In conclusion, we have described the optimal conditions for ultrafast complete inversion of the electronic population of an atomic or molecular four-level ladder system using a full $\pi$-pulse control scheme. We have shown how much trichromatic $\pi$-pulse control is affected by detuning and pulse chirp. Other parameters that can affect the complete population transfer, such as fluctuations in the energy and duration of the pulses or the ionization rate associated to the shortest pulses, needs to be studied for every specific experimental geometry. Our study hence provides a general numerical solution to an intriguing fundamental theoretical problem which has many potential experimental applications to a variety of fields such as (i) spectroscopy and microscopy, (ii) quantum control of chemical and biochemical reactions, (iii) effective generation of UV ultrashort pulses and pumping of UV lasers, and (iv) quantum computing.

## Acknowledgments

Support from the Spanish Ministry of Economy and Competitiveness through FIS2014-51997-R is acknowledged.

## Author Contributions

Carles Serrat conceived and designed the simulations and wrote the paper. Montserrat Corbera and John Afa performed the simulations.

## Conflicts of Interest

The authors declare no conflict of interest.

## References

1. Mukamel, S. *Principles of Nonlinear Optical Spectroscopy*; Oxford University Press: New York, NY, USA, 1995.
2. Wohlleben, W; Buckup, T; Herek, J.L.; Motzkus, M. Coherent control for spectroscopy and manipulation of biological dynamics. *Chem. Phys. Chem.* **2005**, *6*, 850–857.
3. Nielsen, M.A.; Chuang, I.L. *Quantum Computation and Quantum Information*; Cambridge University Press: Cambridge, UK, 2000.
4. Cao, J.; Bardeen, C.J.; Wilson, K.R. Molecular "$\pi$ pulse" for total inversion of electronic state population. *Phys. Rev. Lett.* **1998**, *80*, 1406–1409.
5. Meshulach, D.; Silberberg, Y. Coherent quantum control of multiphoton transitions by shaped ultrashort optical pulses. *Phys. Rev. A* **1999**, *60*, 1287–1292.

6. Hioe, F.T.; Bergmann, K. Adiabatic population transfer in a three-level system driven by delayed laser pulses. *Phys. Rev. A* **1989**, *40*, 6741–6744.
7. Schiemann, S.; Kuhn, A.; Steuerwald, S.; Bergmann, K. Efficient coherent population transfer in NO molecules using pulsed lasers. *Phys. Rev. Lett.* **1993**, *71*, 3637–3640.
8. Bergmann, K.; Theuer, H.; Shore, B.W. Coherent population transfer among quantum states of atoms and molecules. *Rev. Mod. Phys.* **1998**, *70*, 1003–1025.
9. Král, P.; Thanopulos, I.; Shapiro, M. Colloquium: Coherently controlled adiabatic passage. *Rev. Mod. Phys.* **2007**, *79*, doi:10.1103/RevModPhys.79.53.
10. Diels, J.-C. Efficient selective optical excitation for isotope separation, using short laser pulse. *Phys. Rev. A* **1976**, *13*, 1520–1527.
11. Diels, J.-C.; Besnainou, S. Multiphoton coherent excitation of molecules. *J. Chem. Phys.* **1986**, *85*, 6347–6355.
12. Biegert, J.; Diels, J.-C. Feasibility study to create a polychromatic guidestar in atomic sodium. *Phys. Rev. A* **2003**, *67*, doi:10.1103/PhysRevA.67.043403.
13. Serrat, C.; Biegert, J. Energy efficient method for two-photon population transfer with near-resonant chirped pulses. *Opt. Express* **2008**, *16*, 19667–19673.
14. Brewer, R.G.; Hahn, E.L. Coherent two-photon processes: Transient and steady-state cases. *Phys. Rev. A* **1975**, *11*, 1641–1649.
15. Sargent, M., III; Horwitz, P. Three-level Rabi flopping. *Phys. Rev. A* **1976**, *13*, 1962–1964.
16. Shore, B.W.; Ackerhalt, J. Dynamics of multilevel laser excitation: Three-level atoms. *Phys. Rev. A* **1977**, *15*, 1640–1647.
17. Carroll, C.E.; Hioe, F.T. Driven three-state model and its analytic solutions. *J. Math. Phys.* **1988**, *29*, 487–509.
18. Chelkowski, S.; Bandrauk, A.D. Coherent propagation of intense ultrashort laser pulses in a molecular multilevel medium. *J. Chem. Phys.* **1988**, *89*, 3618–3628.
19. Choe, A.S.; Rhee, Y.; Lee, J.; Han, P.S.; Borisov, S.K.; Kuzmina, M.A.; Mishin, V.A. Effective excitation method of a three-level medium in a selective photoionization. *Phys. Rev. A* **1995**, *52*, 382–386.
20. Linskens, A.F.; Holleman, I.; Dam, N.; Reuss, J. Two-photon Rabi oscillations. *Phys. Rev. A* **1996**, *54*, 4854–4862.
21. Kim, J.B.; Lee, J.; Choe, A.S.; Rhee, Y. Geometrical representation of coherent-excitation methods using delayed and detuned lasers. *Phys. Rev. A* **1997**, *55*, 3819–3825.
22. Diels, J.-C.; Rudolph, W. *Ultrashort Laser Pulse Phenomena*; Academic Press—Elsevier: San Diego, CA, USA, 2006.
23. Zhang, B.; Wu, J.-H.; Yan, X.-Z.; Wang, L.; Zhang, X.-J.; Gao, J.-Y. Coherence generation and population transfer by stimulated Raman adiabatic passage and $\pi$ pulse in a four-level ladder system. *Opt. Express* **2011**, *19*, 12000–12007.
24. Sakurai, J. *Modern Quantum Mechanics*, 2nd ed.; Addison-Wesley: Boston, MA, USA, 1993; p. 181.

25. Buckup, T.; Hauer, J.; Serrat, C.; Motzkus, M. Control of excited-state population and vibrational coherence with shaped-resonant and near-resonant excitation. *J. Phys. B At. Mol. Opt. Phys.* **2008**, *41*, doi:10.1088/0953-4075/41/7/074024 .
26. Ziolkowski, R.W.; Arnold, J.M.; Gogny, D.M. Ultrafast pulse interactions with two-level atoms. *Phys. Rev. A* **1995**, *52*, 3082–3094.
27. Wrzesinski, P.J.; Pestov, D.; Lozovoy, V.V.; Gord, J.R.; Dantus, M.; Roy, S. Group-velocity-dispersion measurements of atmospheric and combustion-related gases using an ultrabroadband-laser source. *Opt. Express* **2011**, *19*, 5163–5171.